Design of a Dual-Band Flexible Microstrip Patch Antenna on Transparent Substrate for IoT and ISM Band Applications

Ayush Mukherjee
Electronics and Communication Engineering Dept.
Institute of Engineering and Management
Kolkata, India
supriyamukherjee1979@gmail.com

Subhradip Bal
Electronics and Communication Engineering Dept.
Institute of Engineering and Management
Kolkata, India
bal.subhradb@gmail.com

Satavisha Dutta
Electronics and Communication Engineering Dept.
Institute of Engineering and Management
Kolkata, India
satavishadutta0@gmail.com

Gobinda Sen
Electronics and Communication Engineering Dept.
Institute of Engineering and Management
Kolkata, India
gobinda.sen@iem.edu.in

***Abstract*—The presented work follows a transparent and flexible dual band microstrip-fed patch antenna that can function in both Internet of Things (IoT) and Industrial, Scientific and Medical (ISM) Band applications. The radiating parts of the antenna consist of two inverted L-shaped patches with two slots cut on it fed by a microstrip feedline along with a rectangular stub above it while the ground plane is modified to achieve dual-band functionality. The novelty of the presented work is showcased by the use of low-cost and flexible Polyethylene terephthalate (PET) material, a thermoplastic semi-crystalline polymer of the polyester group has been used as the substrate with dielectric constant taken as 3.6 and a thickness of 1.6 mm, to achieve optical transparency. The antenna is capable of resonating within the frequency bands of 3.56 GHz to 6.73 GHz with an impedance bandwidth span of 0.26 GHz over frequencies of 3.56 GHz to 3.82 GHz and 1.42 GHz over 5.31 GHz to 6.73 GHz. The proposed design of the antenna is simulated using the Ansys HFSS (High Frequency Structure Simulator) software which runs on finite element method (FEM) technique and then finally fabricated.**

Keywords—Antennas, transparent, dual-band, flexible, Polyethylene terephthalate (PET), defected ground structure.

I. INTRODUCTION

The modernization of technologies in the 21st century led to engineering marvels in the design and fabrication of antennas which are being used for Internet of Things (IoT) as well as for Industrial, Scientific and Medical (ISM) bands [1]. The evolution of the antennas are taking place rapidly to accelerate the growth of the industries in relation to the frequencies they resonate in, thus procuring the need of suitable communication systems for error-free data transmission [2].

Transparent electronics have gained an immense popularity these days which are implemented seamlessly across various domains of modern scientific and industrial applications due to their easy integration with the existing communication technologies. The construction of a transparent antenna is structured in such way that it cannot be seen or almost slightly prominent when integrated or placed on glass, plastic or other transparent materials. The usage of these antennas are applicable in areas where the function of traditional design antennas are non-workable and where design factors are considered [3]. Conversely, compared to other conventional antennas, flexible antennas are well-regarded because of their compatible and versatile integration with curved or irregular surfaces, thus finding applications in wide range of substantial communication technologies [4]. Thus the implementation of flexible antenna with transparent substrate finds applications in wide range of wearable technologies because of their almost invisible appearance as well as new aspects of broader features which were previously unimaginable [5]. Transparent electronic systems have enabled seamless discrete implementations of the technological systems. So it will be necessary to upgrade the antennas for modern scientific uses as the size of the gadgets decreases, there will be necessities for antennas that can support huge capacities as well as compatible sizes [6]. In this way, transparent antennas can thus introduce novel features in their usages which were deemed impossible before.

In [7], J. Kaur *et al* proposed a microstrip-fed patch antenna with two inverted radiating patches which are L-shaped and can operate in dual-band frequencies, along with FR-4 epoxy substrate on a defective ground structure. However, the use of flame retardant FR-4 epoxy makes the design unsuitable for wearable applications. Hence in this work, a new design is proposed using a transparent Polyethylene terephthalate (PET) substrate with a transparency of 95%. Along with the radiating parts of the antenna which involve the patches additionally a rectangular stub is placed above the patches and two slots of equal dimensions have been cut on the patches. The usage of PET as material for the substrate supported to the transparency and wearable operability of the antenna. The proposed design operates effectively within the frequency range of 3.56 GHz to 6.73 GHz, exhibiting return losses below -10 dB. It achieves gain values of 4.41 dBi at 3.68 GHz and 5.71 dBi at 5.88 GHz. The impedance bandwidth spans 0.26 GHz between 3.56 GHz and 3.82 GHz, and 1.42 GHz between 5.31 GHz and 6.73 GHz with radiation efficiency of 99%. Thus this design can agreeably be used to operate in the IoT and ISM bands thus offering a large bandwidth. The following sections outline the comprehensive layout of the proposed structure and in-depth analysis of the simulated outcomes including reflection coefficient, radiation pattern, gain, VSWR and surface current distribution alongside the fabricated results.

II. ANTENNA DESIGN

The proposed work comprises a simple monopole antenna which involves two L-shaped radiating patches which are inverted and are fed by a microstrip line of length (L_1) = 5 mm. The longer strips connecting the patches to the feedline are of length (L_2) = 33.5 mm and of thickness (a) = 2 mm. The arms of both the patches are of length (L_3) = 11.7 mm and of width (W_3) = 23 mm and are separated by a gap (b) of 2 mm. The PET material used for the substrate used has a dielectric constant (ε) = 3.6, loss tangent = 0.02 [8] and of thickness (H_s) = 1.6 mm. Additionally, a rectangular stub of length (L) = 40 mm and of thickness (W) = 3 mm has been added at a gap (g) of 0.1 mm from the patches along with two slots of equal dimensions ($L_p \times W_p$) = 6 × 2 mm^2 have been cut on the patches. The ground has been incorporated into a plus-shaped structure (+) with the dimensions of the longer arm ($L_s \times W_{g1}$) = 70 x 31 mm^2 and that of the shorter arm ($W_s \times L_{g1}$) = 60 × 8 mm^2 for improved impedance matching and reduction in unwanted responses.

The dimensions of the antenna, including its length and width, can be determined using the equations provided [9]:

$$W = \frac{1}{2f_r\sqrt{\mu_0\varepsilon_0}}\sqrt{\frac{2}{\varepsilon_r+1}} \quad (1)$$

where f_r stands for the resonant frequency, μ_0 indicates the magnetic permeability in free space, ε_0 corresponds to the electric permittivity in a vacuum and ε_r signifies the substrate's relative permittivity.

$$L = L_{eff} - L \quad (2)$$

where L_{eff} represents the patch's effective length expressed as:

$$L_{eff} = \frac{c}{2f_r\sqrt{\varepsilon_{eff}}} \quad (3)$$

where ε_{eff} is effective relative permittivity given as follows:

$$\varepsilon_{eff} = \frac{\varepsilon_r+1}{2} + \frac{\varepsilon_r-1}{2}\left(1+\frac{12h}{W}\right)^{-\frac{1}{2}} \quad (4)$$

and L is the length extension given as follows:

$$L = 0.412h\frac{(\varepsilon_{eff}+0.3)\left(\frac{W}{h}+0.264\right)}{(\varepsilon_{eff}-0.258)\left(\frac{W}{h}+0.8\right)} \quad (5)$$

The complete geometry of the proposed antenna along with modified ground structure is given in Fig.1 (a)-(b).

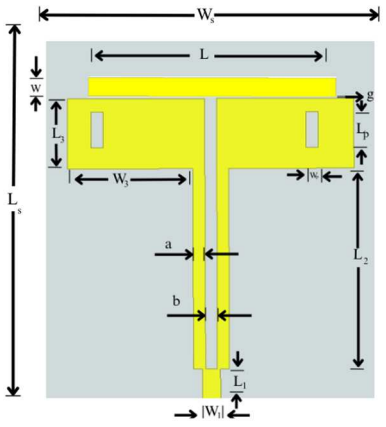

(a)

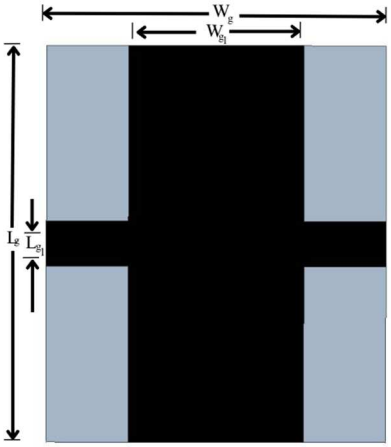

(b)

Fig. 1. a) Top view of the proposed design
b) Back view of the modified ground structure

The addition of the rectangular stub at the distance of 0.1 mm from the patches have an impacted wideband effect on the design thus giving better gain for the results. It has also been noted that introducing two slots on the patches affects the antenna's performance, thus offering sufficient amount of reflection coefficients for the desired resonating frequencies in the applicable IoT and ISM bands. The defective ground structure of the antenna with the modified design contribute to the reduction of mutual coupling and better surface current control, thus eventually improving the impedance matching, minimizing reflection and ensuring more and efficient power transmission.

The following parameters show in Table I are used in designing the proposed antenna.

TABLE I. DIMENSIONS OF THE ANTENNA

Parameter	Value (mm)	Parameter	Value (mm)
L_1	5	W_p	2
W_1	3	L_s	70
L_2	33.5	W_s	60
W_2	2	H_s	1.6
L_3	11.7	L_{g1}	8
W_3	23	W_{g1}	31
L	40	a	2
W	3	b	2
L_p	6	g	0.1

III. RESULTS AND ANALYSIS

The outcomes of the design of the antenna are analyzed through simulations conducted on Ansys HFSS (High Frequency Structure Simulator) software which employs FEM (Finite Element Method) to assess the impact of the design parameters.

A. Simulated Results

The proposed design resonates at frequencies around 3.68 GHz and 5.88 GHz exhibiting reflection coefficients of around -17.47 dB and -32.46 dB. Thus this design resonates at dual band frequencies with a common operating impedance bandwidth of 0.26 GHz and 1.42 GHz over a span of 3.56 GHz to 3.82 GHz and 5.31 GHz to 6.73 GHz respectively in the IoT and ISM bands. This result shows an improvement from the standard FR4-epoxy as substrate. Fig. 2 illustrates the design's reflection coefficient obtained from simulation.

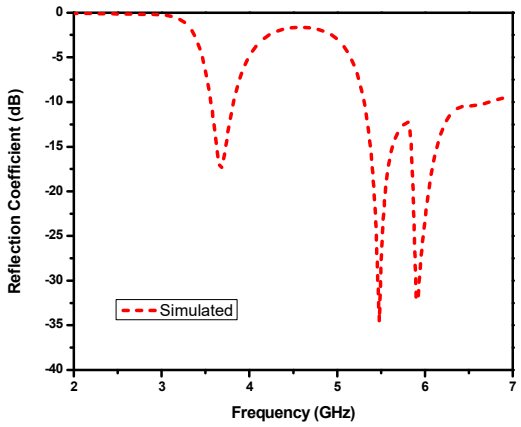

Fig. 2. Reflection coefficient plot of the proposed design

The radiation pattern depicts the way an antenna's total energy is distributed directionally. The angular dispersion of the radiation is also influenced by the E-plane and H-plane radiation patterns, thus making it crucial to judge an antenna with good directivity. Another critical parameter is the gain which shows how efficiently the antenna radiates energy in specific directions in comparison to an ideal reference antenna. The polar plots in Fig. 3 (a)-(b) illustrates the simulated radiation pattern outcomes for E-plane (Phi = 0°) and H-plane (Phi = 90°) at 3.68 GHz and 5.88 GHz.

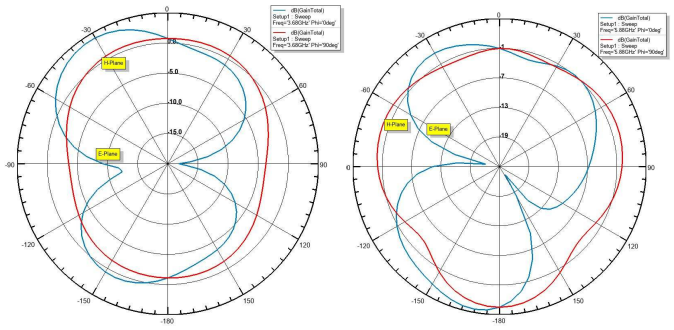

(a) (b)

Fig. 3. Radiation pattern of the antenna at (a) 3.68 GHz, and (b) 5.88 GHz

The antenna delivers gains of 4.41 dBi at 3.68 GHz and 5.71 dBi at 5.88 GHz, respectively, thus showing the effect of transparent PET material over the conventional FR-4 material being used as substrate for the design. The E-plane and the H-plane radiation patterns indicate good agreement of the gain with the resonating frequencies.

The degree to which the impedance is matched between the source and the feed point is measured by the Voltage Standing Wave Ratio (VSWR). The VSWR, depicted by Fig. 4 shows the acceptable performance of the design which is less than 2 thus resulting lower directivity of the proposed design.

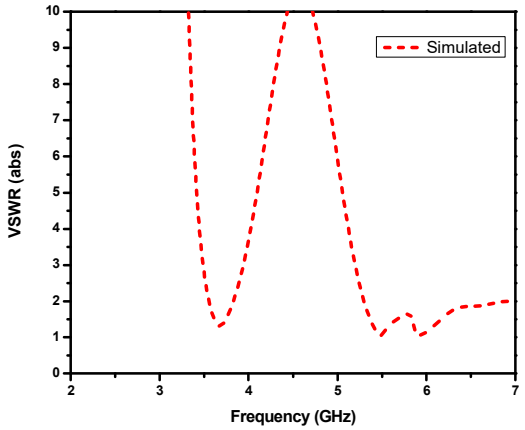

Fig. 4. Simulated VSWR Plot

Using current distribution on the surface of the patches and the rectangular stub, which refers to the variation of electric current across it, the float of current for a specific resonant frequency can be calculated. Fig. 5 (a)-(b) illustrates the surface current distribution for the two bands of frequencies 3.68 GHz and 5.88 GHz, on the patches and the stub.

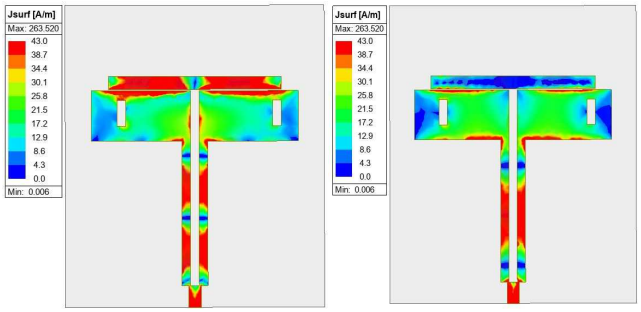

(a) (b)

Fig. 5. Surface current distribution of the patch and the stub for a) 3.68 GHz and b) 5.88 GHz

B. Experimental Verification

The proposed design is fabricated with slight optimization in the thickness of the transparent substrate as depicted in Fig. 6 (a)-(b) and experimental results as obtained from Anritsu MS46122B020 series VNA in an anechoic chamber (in Fig. 8 (a)-(b)) are verified with the simulated one in Fig. 9. However, the measured plot, which represents the performance of the fabricated antenna, shows a slight shift at the resonating frequencies due to manual fabrication inaccuracy. Other parameters such as dimensions of the substrate, patch and the stub, along with the modification of the ground plane into a defective structure to provide efficiency in the results, have been kept intact.

TABLE II. COMPARISON OF PARAMETERS OF DIFFERENT TRANSPARENT ANTENNAS

Design	Frequency	Gain (dBi)	Bandwidth (%)	Radiation Efficiency (%)	Substrate Material Used	Transparency (%)
Proposed	3.56– 3.82 GHz, 5.31 – 6.73 GHz	4.41 , 5.71	7.05 , 23.59	99	PET	95
[10]	2.2 – 25 GHz	3.2, 4.3, 3.7, 4.5	-10 dB	75	PDMS	70
[11]	4.9 GHz	5.16	-10 dB	90	Soda lime glass	60
[12]	2.47 GHz, 5.32 GHz	0.64, 1.2	7.15, 2.42	62, 83	Borosilicate glass	80

(a) (b)

Fig. 6. Fabricated antenna design (a) Front view (b) Back view

Despite the difference in the shifts, the resonant frequency in both plots is very close, with only a minimal shift is observed. This demonstrates that the fabricated antenna closely replicates the simulated design, effectively meeting the requirements of the desired frequency bands along with the usage of its applications.

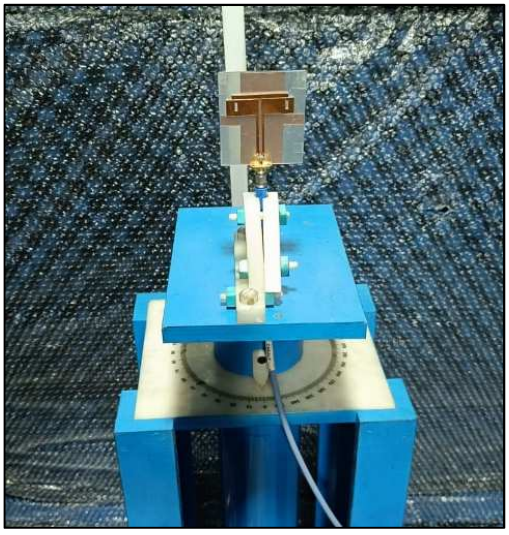

Fig. 7. Frontal view of the antenna attached

Table II provides a comparative overview of several transparent antennas developed using various substrate materials namely polydimethylsiloxane (PDMS) [10], soda lime glass [11] and borosilicate glass [12], alongside the proposed design. The comparison encompasses key performance parameters such as gain, bandwidth, radiation efficiency, and optical transparency. The results clearly highlight the superior performance of the proposed antenna, which utilizes PET as a substrate, demonstrating notable improvements across multiple metrics. This underscores the effectiveness and suitability of the PET-based design for advanced transparent antenna applications.

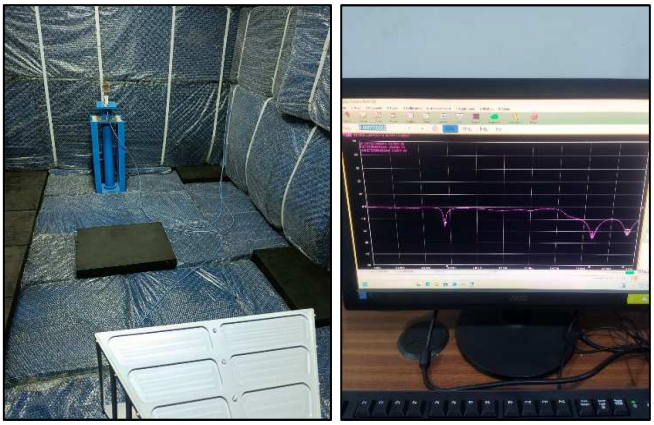

(a) (b)

Fig. 8. Experimental setup of the proposed design at a) Anechoic chamber and b) measurement results

The novelty of the fabricated structure is showcased by incorporating PET sheet as substrate along with copper strips for the patch and the ground. This not only enhances the design's transparency but also adds flexibility and wearability. The antenna not only gives a good VSWR reading for the resonant frequencies along with low directivity, but it also boasts a very high radiation efficiency of 99%. These parameters contribute to the high performance attained by the design during its usage.

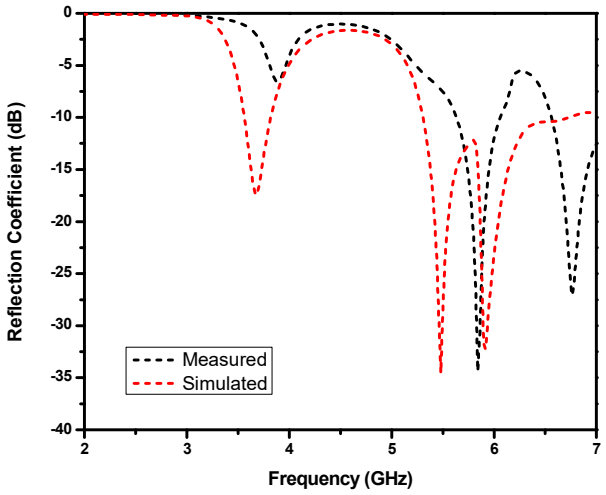

Fig. 9. Measured and Simulated Reflection Coefficient Plot

IV. CONCLUSION

The presented work features the design and proper fabrication of a versatile dual-band microstrip patch antenna with an optically transparent PET substrate on a defected ground structure. The antenna operates between the frequencies of 3.56 GHz and 6.73 GHz with gain of 4.41 dBi and 5.71 dBi at 3.68 GHz and 5.88 GHz, thus making it suitable to work in the IoT and ISM bands and also covering the agreeable amount of bandwidth. The use of PET is characterized by its low-cost production and compactness to achieve optical transparency as well as visual aesthetic of the design. Besides these, PET also offers toughness and high glass transition temperature [13]. Also PET substrate is used for human-body wearable applications due to its low-cost, transparent and flexible features [14]. Furthermore, the material's sustainable nature contributes to its high recyclability and low energy requirements during production, enhancing its environmental friendliness [15]. Nowadays many transparent antennas with various conductive metal materials as conductive layers are being designed and fabricated, leading to new insights into materials and communication engineering [16]. This work can also considered to be another step in exploring the results and effectiveness of transparent antennas using various transparent substrates [17]. Further, more research can be carried out to discover new applications for these type of antennas in the future endeavor.

REFERENCES

[1] A. S. MD. Sayem, A. Lalbakhsh, K. P. Esselle, J. L. Buckley, B. O' Flynn, R. B. V. B. Simorangkir, "Flexible Transparent Antennas: Advancements, Challenges, Prospects," *IEEE Open Journal of Antennas and Propagation*, vol. 3, pp. 1109-1133, Sept 2022.

[2] D. Mollik, R. Islam, A. B. Anwar, P. K. S. Purnendu, M. A. H. Shanto and M. Ahmad, "Design of 24 GHz ISM Band Microstrip Patch Antenna for 5G Communication," *2022 IEEE International IOT, Electronics and Mechatronics Conference (IEMTRONICS)*, Toronto, ON, Canada, 2022, pp. 1-6, doi: 10.1109/IEMTRONICS55184.2022.9795716.

[3] E. C. Patil, S. D. Lokhande, U. A. Patil, A. U. Patil, J. Kumar. (2024, January). "Optically transparent dual-band antenna for UHF and S-band applications." *Optical Materials* [Online]. vol. 147. Available: https://www.sciencedirect.com/science/article/abs/pii/S0925346723011874?via%3Dihub

[4] A. Ericsson, "Cellular networks for massive IoT-enabling low-powered wide area applications, Ericsson, Stockholm, Sweden, Rep. UEN 28423-3278, Jan. 2016.

[5] J. Kim *et al*., "Wearable smart sensor systems integrated on soft contact lenses for wireless ocular diagnostics," *Nat. Commun*,. vol. 8, no. 1 Apr. 2017, Art. No. 14997.

[6] F. Boccardi, R. W Heath, A. Lozano, T. L. Marzetta and P. Popovski, "Five disruptive technology directions for 5G," *IEEE Commun. Mag.*, vol. 52, no. 2, pp. 74-80, Feb.2014.

[7] J. Kaur, R. Khanna, "Development of Dual-band Microstrip Patch Antenna For WLAN/MIMO/WiMAX/AMSAT/WAVE Applications". *Microwave and Optical Technology Letters* [Online]. vol. 56, no. 4. DOI 10.1002/mop

[8] M. Knitter, E. Markiewicz, J. Jurga. (2010). "Dielectric Properties of Polyethylene Terephthalate/ Polyphenylene Sulfide/Barium Titanate Nanocomposite for Application in Electronic Industry," *Polymer Engineering & Science* [Online]. vol. 50, no. 8, 1613-1619, 2010

[9] K. Prajapati and P. K. Patidar, "Design and Analysis of 4 X 4 Microstrip Patch Antenna Array with DGS for 5G Communication Applications," ijrim.com, 2021, [Online]. Available: https://ijrim.com/Admin/uploads/Final_Paper_10.pdf

[10] Y. Zhang, S. Shen, C.Y. Chiu, and R. Murch, "Hybrid RF-solar energy harvesting systems utilizing transparent multiport micromeshed antennas," *IEEE Trans. Microw. Theory Techn*., vol. 67, no. 11, pp. 4534-4546, Nov. 2019.

[11] A. S. Thampy and S.K. Dhamodharan, "Performance analysis and comparison of MWCNT loaded ITO and TIO based optically transparent patch antennas for terahertz communications," *Phys. E: Low-dimensional Syst. Nanostruct.,* vol. 66, pp. 52-58, Feb. 2015.

[12] W. Hong, S. Lim, S. Ko, and Y. G. Kim, "Optically invisible antenna integrated within an OLED touch display panel for IoT applications," *IEEE Trans. Antennas Propag*., vol. 65, no. 7, pp. 3750-3755, Jul. 2017.

[13] M. S. V. Ferreira, S. H. Mousavi. (2018, April). "Nanofiber technology in the ex vivo expansion of cord blood-derived hematopoietic stem cells". *Nanomedicine: Nanotechnology, Biology, and Medicine* [Online]. vol. 14, issue 5, pp. 1707-1718. Available: https://doi.org/10.1016/j.nano.2018.04.017

[14] K. Upreti, "A Flexible Wearable Antenna for Wireless Body Area Network Application," 2021 IEEE Indian Conference on Antennas and Propagation (InCAP), Jaipur, Rajasthan, India, India, 2021, pp. 163-166, doi: 10.1109/InCAP52216.2021.9726475.

[15] T. M. Joseph *et al.* (2024). "Polyethylene terephthalate (PET) recycling: A review," *Case Studies in Chemical and Environmental Engineering* [Online]. vol. 9. Available: https://doi.org/10.1016/j.cscee.2024.100673

[16] Z. J. Silva, C. R. Valenta and G. D. Durgin, "Optically Transparent Antennas: A Survey of Transparent Microwave Conductor Performance and Applications," in *IEEE Antennas and Propagation Magazine*, vol. 63, no. 1, pp. 27-39, Feb. 2021, doi: 10.1109/MAP.2020.2988526.

[17] O. R. Alobaidi, P. Chelvanathan, S. K. Tiong, B. Bais, MD. A. Uzzaman, N. Amin. (2022, February). "Transparent Antenna for Green Communication Feature: A Systematic Review on Taxonomy Analysis, Open Challenges, Motivations, Future Directions and Recommendations". *IEEE Access* [Online]. vol. 10, pp. 12286-1232. DOI: 10.1109/ACCESS.2020.3044435.